A R M S T R O N G   L A B O R A T O R Y
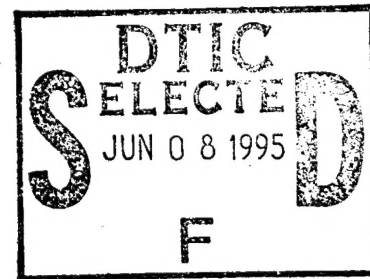
LASER-INDUCED ACOUSTIC AND SHOCK WAVES IN OCULAR TISSUES

Alexander A. Oraevsky

TASC, Inc.
750 East Mulberry, Suite 302
San Antonio, Texas 78212-3159

DTIC
SELECTED
JUN 0 8 1995
F

OCCUPATIONAL AND ENVIRONEMNTAL HEALTH DIRECTORATE
Optical Radiation Division
8111 18th Street
Brooks Air Force Base, Texas 78235-5215

May 1995

Final Technical Report for Period January - August 1994

19950605 049

DTIC QUALITY INSPECTED 3

AIR FORCE MATERIEL COMMAND
BROOKS AIR FORCE BASE, TEXAS

REPORT DOCUMENTATION PAGE

1. AGENCY USE ONLY *(Leave blank)*	2. REPORT DATE May 1995	3. REPORT TYPE AND DATES COVERED Final – Jan 94 – Aug 94

4. TITLE AND SUBTITLE

Laser-Induced Acoustic and Shock Waves in Ocular Tissues

5. FUNDING NUMBERS

C – F33615-92-C-0017
PE – 62202F
PR – 2312
TA – A1
WU – 01

6. AUTHOR(S)

Alexander A. Oraevsky

7. PERFORMING ORGANIZATION NAME(S) AND ADDRESS(ES)

TASC, Incorporated
750 E. Mulberry
Suite 302
San Antonio, TX 78212-3159

8. PERFORMING ORGANIZATION REPORT NUMBER

9. SPONSORING/MONITORING AGENCY NAME(S) AND ADDRESS(ES)

Armstrong Laboratory
Occupational and Environmental Health Directorate
Optical Radiation Division
8111 18th Street
Brooks Air Force Base, Texas 78235-5215

10. SPONSORING/MONITORING AGENCY REPORT NUMBER

AL/OE-TR-1995-0044

11. SUPPLEMENTARY NOTES

12a. DISTRIBUTION/AVAILABILITY STATEMENT

Approved for public release; distribution is unlimited.

12b. DISTRIBUTION CODE

13. ABSTRACT *(Maximum 200 words)*

Analytical expressions that describe the generation and propagation of acoustic and shock waves in biological tissues are presented. Several practical situations of laser irradiation of various ocular tissues have been considered and these include thermoelastic generation of acoustic waves, linear and nonlinear effects that occur upon propagation of stress transients in tissues, cylindrical shock wave generation upon plasma optical breakdown in the caustic of a focused laser beam, and spherical shock wave generation upon thermal explosion of melanosomes. The transformation of light energy into heat and then to mechanical stress is analyzed for ultrashort-pulse laser irradiation of absorbing tissues, and thermo-optical generation of high-amplitude acoustic waves and the formation of shock waves are reviewed. Stress wave alteration upon propagation through various media is considered along with acoustic wave reflection from boundaries and acoustic wave transmission through interfaces. Finally, nonlinear propagation of high-amplitude acoustic waves is covered.

14. SUBJECT TERMS

Melanosomes; Ocular tissues; Shock wave; Ultrashort pulse

15. NUMBER OF PAGES

16. PRICE CODE

17. SECURITY CLASSIFICATION OF REPORT	18. SECURITY CLASSIFICATION OF THIS PAGE	19. SECURITY CLASSIFICATION OF ABSTRACT	20. LIMITATION OF ABSTRACT
Unclassified	Unclassified	Unclassified	UL

TABLE OF CONTENTS

Accesion For

NTIS CRA&I	☑
DTIC TAB	☐
Unannounced	☐
Justification	

By

Distribution /

Availability Codes

| Dist | Avail and / or Special |

A-1

iii

FIGURES

GENERATION AND PROPAGATION OF ACOUSTIC AND SHOCK WAVES IN OCULAR TISSUES (THEORY)

INTRODUCTION

Analytical equations that describe generation and propagation of acoustic and shock waves in biological tissues are presented. Several practical situations of laser irradiation of various ocular tissues are considered: thermoelastic generation of acoustic waves, linear and nonlinear effects that occur upon propagation of stress transients in tissues, cylindrical shock wave generation upon plasma optical breakdown in the caustic of a focused laser beam, and spherical shock wave generation upon thermal explosion of melanosome.

Laser irradiation of ocular tissues can lead to the following two major types of physical processes: heat generation and an optical breakdown. It is tissue absorption coefficient and laser intensity that determine the type of laser-tissue interaction mechanisms. In cases where tissue is strongly absorbing and laser radiation is not strongly focused in a medium, fast nonradiative relaxation of the excited states converts absorbed laser energy into heat. Also, when tissue is transparent for the laser light, the only process that allows laser energy to be deposited in tissue is plasma optical breakdown by the high electric field in a focused laser beam. Optical breakdown can also occur when strongly absorbing tissue is superheated to a temperature of several thousand degrees.

Generation of acoustic waves by the consecutive transformation of light energy into heat and then to mechanical stress is the most essential phenomenon upon short-pulse laser irradiation of absorbing tissues. Thermooptical generation of acoustic waves of high amplitude and formation of shock waves because of nonlinear propagation in various materials have been investigated and reviewed in the literature.[1-10] Short laser pulses allow the most efficient realization of thermoelastic stress induction because of minimal stress relaxation during laser heating (see also section on Stress Relaxation). There are a number of publications devoted to various mechanisms of generation and propagation of short-pulse, laser-induced shock waves in water containing tissues.[11-14] Plasma optical breakdown in water and water containing tissues has been experimentally investigated (see, for example, publications by Vogel[11] and Docchio.[15]) However, theoretical considerations of optical breakdown are not as thorough as experimental studies.

Existing literature is lacking analytical equations which may allow simple estimations of acoustic-mechanical effects of laser pulses on ocular tissues. Unfortunately, analytic solutions of thermodynamic equations can not be obtained in many general cases that describe laser induced acoustic and shock waves.

GENERATION AND PROPAGATION OF ACOUSTIC AND SHOCK WAVES

Laser-induced Thermoelastic Stress

Let us consider an interaction of a laser pulse with soft biological tissue with properties close to that of water. Let irradiance incident to the tissue surface be:

$$I(x, y, t) = I(x, y)L(t) \qquad (1)$$

where L(t) is the normalized time-function that defines the temporal profile of the laser pulse ($0 < L(t) < 1$). The characteristic duration of laser pulse is τ_L. The spatial distribution of a laser beam usually has a Gaussian profile in the x-y plane

$$I(x, y) = I_o \exp\left[-(x^2 + y^2)/a^2\right] \qquad (2)$$

where a is the characteristic radius of the laser beam. Let the laser radiation propagate along the z-axis. Because a laser beam radius is substantially smaller compared to the dimensions of irradiated tissue, we may assume that tissue is infinite in dimensions and occupies the half space z>0.

The pressure distribution (a Laplasian pressure) in tissue can be described by the wave equation:

$$\Delta P - \frac{1}{C_s^2} \frac{\partial^2 P}{\partial t^2} = \frac{\beta}{C_p} \frac{\partial Q}{\partial t} \qquad (3)$$

where P is the pressure, C_S is the speed of sound, t is time, β is the volume coefficient of thermal expansion, C_P is the heat capacity at constant pressure, Q is the spatial and temporal profile of heat distribution.

$$Q(x, y, z, t) = T\mu_a I(x, y) \exp(-\mu_{eff} z)L(t) \qquad (4)$$

where T is the optical transmittance through the tissue boundary dependent on the specular reflection coefficient and the shape of tissue surface, μ_a is the tissue absorption coefficient, and μ_{eff} is the effective attenuation coefficient.

Stress Transients in the Far Zone

An analytic solution of Equation (3) can be found outside the optical zone in the region located at the distance R>>a, μ_a^{-1}. Acoustic pressure in this case can be expressed in a very general case of laser irradiation as:[3]

2

$$P = -\frac{T\beta a^2 I_0}{4\pi C_p R \tau_\mu^2} \int_o^\infty \exp\left(-\frac{k^2 S^2}{4}\right) \frac{k^2}{1+k^2} \exp(ik\gamma) F\left(\frac{k}{\tau_\mu}\right) dk \qquad (5)$$

where we introduced the following symbols: $k = \omega \tau_\mu$, $\gamma = (R/C_S - t) \tau_\mu^{-1}$, $S = \tau_a/\tau_\mu$, R is the distance from center of our coordinate system to the observation point, $\tau_\mu = \cos\theta/\mu_a C_S$, and $\tau_a = a \sin\theta/C_S$ are characteristic delay times for the ultrasound waves propagating from elementary sources in the z-direction and in the x-y (surface) plane respectively, θ is the angle between the z-axis and the direction to the point of observation, $F(\omega)$ is the acoustic spectrum of laser-induced stress transients after the end of laser pulse, and ω is the modulation frequency of laser intensity. Laser pulse spectrums can be expressed as follows:

$$F(\omega) = \int_o^\infty L(t) \exp(i\omega t) dt \qquad (6)$$

Let us consider various limit cases when one can neglect the delay between moments of acoustic wave arrival time to the point of observation from elementary sources located along the z-axis of laser incidence (τ_L relative to τ_μ) and in the plane perpendicular to the laser beam (τ_L relative to τ_a).

(1) In the case when $\tau_L \gg \tau_a$ and $\tau_L \gg \tau_\mu$ Equation (5) can be given as:

$$P(z) = -\frac{T\beta a^2 I_0}{4\pi C_p R \tau_\mu} \bullet \frac{\partial^2 L}{\partial\left(t - \frac{R}{C_S}\right)^2} \qquad (7)$$

In this case the profile of laser-induced stress transient has characteristic M-shape (the second differential from a bell-shaped laser pulse), and its parameters do not depend on laser intensity distribution over the surface (x-y) plane.

(2) In the case when $\tau_L \gg \tau_a$ and $\tau_L \ll \tau_\mu$ the irradiated volume with heat sources has the shape of an elongated cylinder. The Equation (5) can be presented in this case for a **narrow laser beam** as:

$$P(z) = -\frac{T\beta a^2 I_0}{4\pi C_p R \tau_\mu} \left\{ L\left(t - \frac{R}{C_S}\right) - \pi \frac{F*(\omega)}{\tau_\mu} \exp\left(-/t - \frac{R}{C_S}/\right) \right\} \qquad (8)$$

3

where $F^*(\omega)$ in this case is just an integral over the pulse temporal profile,

$$F^*(\omega) = \int_0^\infty L(t)dt.$$

For long laser pulses with duration $\tau_L \gg \tau_a$ the transient stress temporal profile does not depend on the stress relaxation ratio $S = \tau_a/\tau_\mu$ but is determined by the temporal profile of the laser pulse, $L(t)$.

(3) $\tau_\mu \ll \tau_L \ll \tau_a$.

Let us now consider the case of short laser pulses, when heat generation time is shorter compared with stress propagation time along the tissue surface, but not along optical attenuation depth. In this case the equation for acoustic pressure can be given as:

$$P = -\frac{T\beta a^2 I_0}{16 C_p R \tau_\mu^2} F^*(\omega) \bullet \left\{ \frac{4}{\sqrt{\pi}S} \exp\left(\frac{\gamma^2}{S^2}\right) - \exp\left(\frac{S^2}{4}\right) \bullet \left[\exp(-\gamma)erf\left(\frac{s}{2}+\frac{\gamma}{s}\right) + \exp(\gamma)erf\left(\frac{s}{2}-\frac{\gamma}{s}\right) \right] \right\} \quad (9)$$

where $erf(z) = \frac{2}{\pi} \int_z^\infty \exp(-t^2)dt.$

In the case of confined stress conditions of irradiation with a **wide laser beam,** the z-axial profile of laser-induced stress is independent on the temporal profile of the laser pulse and is defined by the stress relaxation ratio, S. Two limit cases can be considered.

(a) Laser irradiated volume (the region of heat sources) has a shape of a flat disk. In this case $S \gg 1$ and Equation (9) can be modified as:

$$P = -\frac{T\beta a^2 I_o}{\sqrt{\pi} c_p R \tau_\mu^2 S^3} F^*(\omega) \bullet \left[\frac{2\left(t-\dfrac{R}{C_s}\right)^2}{\tau_a^2} - 1 \right] \exp\left[-\frac{\left(t-\dfrac{R}{C_s}\right)^2}{\tau_a^2} \right] \quad (10)$$

(b) Laser irradiated volume (the region of heat sources) has a shape of an elongated cylinder. In this case $S \ll 1$ and Equation (9) can be given as:

$$P = -\frac{T\beta a^2 I_o}{8 c_p R \tau_\mu^2 S} F^*(\omega) \bullet \left\{ \frac{2}{\sqrt{\pi}} \exp\left[-\frac{\left(t-\dfrac{R}{C_s}\right)^2}{\tau_a^2} \right] - S \exp\left[-\frac{/t-\dfrac{R}{C_s}/}{\tau_\mu} \right] \right\} \quad (11)$$

4

Practical note: The above given equations are applicable in certain ranges of observation angles.

Equation Number	Observation Angle Range	Equation Number	Observation Angle Range
(7)	$30 \leq \theta \leq 70$	(10)	$60 \leq \theta \leq 90$
(8)	$0 \leq \theta \leq 45$	(11)	$30 \leq \theta \leq 60$

(4) $\tau_L \ll \tau_a$ and also $\tau_L \ll \tau_\mu$

In the case of flat disk geometry of irradiation ($\mu_a \gg a$) with a short laser pulse when not only $\tau_L \ll \tau_a$, but also $\tau_L \ll \tau_\mu$, Equation (5) for the temporal distribution of the pressure wave can be solved analytically as:

$$P(t) = \left(\frac{E_o \beta C_S a^2 \tau_\mu}{2\pi R \tau_a^2} \right) \frac{\partial^2 F}{\partial y^2} \bigg|_{y'} \tag{12}$$

where E_o is the laser pulse energy, and $y' = (C_s t - R)/\sin\theta$ is the distance on the y-axis chosen in the direction of projection of the observation point on the tissue boundary, and $F(y) = \int I(x,y)dx$ is the function that characterizes the effective distribution of elementary heat sources along the y-axis.

Stress Transients in the Near Zone

Characteristic features of acoustic transient pulses, induced by laser pulses in the near zone, can be obtained from the consideration of a simple one-dimensional model.

Let the energy E_{abs} be absorbed in a sphere with radius r_o (assume melanosome).

Sphere. When $r_o \gg c_s \tau_L$ the maximal pressure value in the spherical acoustic wave is:

$$P = \frac{3}{16\pi} \bullet \frac{E_{abs} \beta C_s^2}{C_p r_o^2 R} \tag{13}$$

In this case, amplitude of pressure is determined by the absorbed energy, and the acoustic pulse duration is equal to r_o/c_s.

When $r_o \ll c_s \tau_L$ the maximum pressure value equals:

5

$$P = \frac{3}{16\pi} \bullet \frac{E_{abs}\beta C_S}{C_p r_o R \tau_L} \tag{14}$$

In this case, pressure amplitude is determined by the rate of thermal energy deposition, and acoustic pulse duration is equal to the laser pulse duration. If the irradiated volume has an acoustic impedance mismatch with the medium around it, the temporal profiles of laser-induced acoustic waves have characteristic N-shape (compression pulse followed by the rarefaction pulse).

The efficacy of the thermo-optical mechanism of stress generation in absorbing sphere is described by the equation:

$$\eta_S \cong \frac{1}{4}\left(\frac{\beta C_s}{C_p}\right)^2 \frac{Q}{\rho} \tag{15}$$

Flat Disk. Let the energy E_{abs} be absorbed in a flat disk with thickness equal to $1/\mu_{eff}$ (assume relatively wide laser beam incident on the layer of pigmented epithelium). Thermal expansion of the instantaneously heated medium causes a pressure-rise, P_o, in the irradiated volume. This pressure is proportional to the thermal coefficient of volume expansion, $\beta[K^{-1}]$, of the given medium:

$$P_o = (1/\gamma)\Delta V / V = (1/\gamma)\beta\Delta T \tag{16}$$

where γ [bar^{-1}] is thermodynamic coefficient of isothermal compressibility:

$$\gamma = (C_p / C_v) * (1/\rho) \tag{17}$$

Substituting the Equation (17) for the temperature rise, ΔT

$$\Delta T = E_{abs}(z)/\rho C_v \tag{18}$$

one can get maximal pressure magnitude expressed as:

$$P_O = (\beta C_S^2 / C_p)\Phi_0\mu_a = \Gamma\Phi_0\mu_a \tag{19}$$

where C_s [cm/s] is the sound velocity in medium, ΔV[cm^3] is the volume increase caused by the thermal expansion, V is the laser-irradiated volume initially at room temperature, ρ[g/cm^3] is the tissue density, C_p [J/gK] is the heat capacity at constant pressure, C_v is the heat capacity at constant volume, E_{abs} [J/cm^3] is the absorbed energy density, Φ_o [J/cm^2] is the laser energy fluence incident at the absorbing medium, and μ_a [cm^{-1}] is the absorption coefficient of the ocular tissue.

6

The efficacy of the thermooptical mechanism of stress generation for the flat disk geometry is described by the expression similar to that for a sphere except a numerical factor.

$$\eta_d = \frac{1}{2}\left(\frac{\beta C_s^2}{C_p}\right)\frac{Q}{\rho} \tag{20}$$

The expression ($\beta\ C_s^2/C_p$) in Equation (20) represents the Grüneisen parameter, Γ, which is proportional to the fraction of heat that generates mechanical stress. The value of the Γ-parameter of water and aqueous solutions equals 0.11 at 20° C and rises to 0.125 at 25° C and to 0.5 at 100° C.

Figure 1 shows Grüneisen coefficient as a function of temperature for water and some biological tissues. Linear dependence that is accurate for water is assumed to be valid for water-containing tissues.
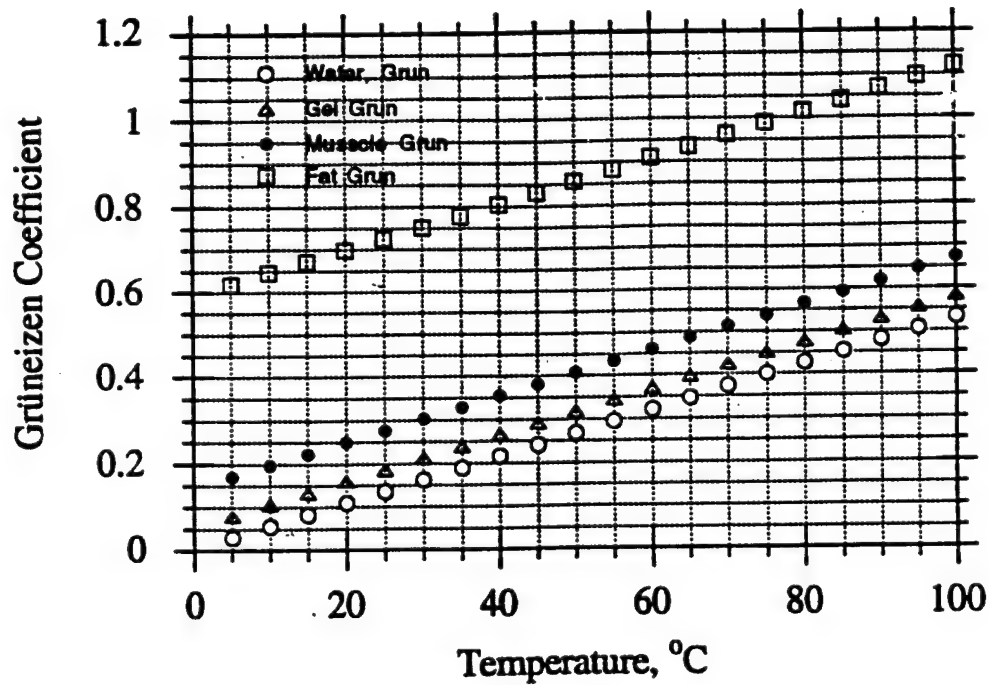
FIGURE 1. G factor for water and tissues as a function of temperature.

Shock Wave Generation upon Plasma Optical Breakdown
on the Surface of Pigment Epithelium

The interaction of an intense short laser pulse with the surface of pigmented epithelium is discussed below. Optical breakdown and formation of a plasma cavity can be observed upon high-intensity, short-pulse irradiation.[11-15] Expansion of the plasma cavity at the end of a laser pulse can give rise to an intense pressure pulse in ambient water of ocular tissue. In many cases, the plasma cavity has a cylindrical shape. Therefore, expansion of the plasma cavity leads to the formation and propagation of cylindrical shock waves in ocular tissues containing water. Subretinal and preretinal hemorrhages and mechanical disruption of intraocular tissues were observed and investigated as a result of optical breakdown reported from numerous studies.[16-20]

Shock Waves from Cylindrical Plasma-Cavity

Let us consider plasma-channel (plasma-cavity) formation with the shape of an elongated cylinder with initial radius $R_i \sim 10^{-3}$ cm and length, L, as a result of pulsed laser heating. We assume that low temperature plasma with initial temperature of $T_i \sim (5 - 15)$ 10^3 K and pressure $P_i \sim 10^2$-10^5 bar is generated in the optical breakdown.

Laser energy absorbed by the plasma will be spent for the increase of plasma internal energy and the work of plasma-cavity expansion:

$$\frac{dW}{dt} + P\frac{dV}{dt} = \frac{dE}{dt} \tag{21}$$

or

$$W(t) + A(t) = E(t) \tag{22}$$

where $V = S L = \pi R^2 L$ is the volume of cylindrical plasma-cavity with radius R, $E=E_{abs}$ is the absorbed laser energy.

Because plasma is relatively low density, the internal plasma energy, W, can be approximated with the equation for the energy of the ideal gas:

$$W = \frac{PV}{\gamma - 1} \tag{23}$$

where γ is the adiabatic parameter of ideal gas.

8

For plasma formed from water at temperatures about 10^4 K, which correspond to the first ionization energy threshold for water, the value of adiabatic parameter γ **equals 1.26.**

The work, $W_{expansion}$, necessary for the plasma-cavity expansion is equal to:

$$W_{exp\,ansion} = \int_{R_i}^{R} Plds \tag{24}$$

Internal homogeneous pressure in the plasma channel is determined by the solution of the system of equations, which describes the plasma channel expansion in ambient water (of ocular tissue) using the Kirkwood-Bethe model with initial and boundary conditions:

$$\frac{du}{dt}\left(1 - \frac{u}{c'_s}\right) + \frac{3}{2}\frac{u^2}{R}\left(1 - \frac{1}{3}\frac{u}{c'_s}\right) = \frac{1}{2}\frac{H}{R}\left(1 + \frac{u}{c'_s}\right) + \left(1 - \frac{u}{c'_s}\right)\frac{1}{c'_s}\frac{dH}{dt} \tag{25}$$

$$H = \frac{c_s^2}{n-1}\left[\left(\frac{P+B}{A}\right)^{\frac{n-1}{n}} - 1\right] = \int_{P_i}^{P}\frac{dP}{\rho} \tag{26}$$

$$P = A\left(\frac{\rho'}{\rho}\right)^n - B \tag{27}$$

where $u = \dfrac{dR}{dt}$ is the rate of plasma-channel expansion, C_s and C'_s are respectively speed of sound in undisturbed water with density ρ and speed of sound in water (with density ρ') exposed to a stress, H is the enthalpy, and A, B, and n are empirical constants (see also Equation (81) in the section titled Formation of a Shock Wave from High Amplitude Acoustic Waves).

The system (Equations 25, 26, 27) accounts for the influence of liquid compressibility when expansion channel velocity is substantial and is approximately equal to the speed of sound in water, C_s. This system of equations can be integrated numerically and shock wave amplitude in ambient water can be obtained if the equation for the energy deposition E(t) is known.

Some simple estimates of hydrodynamic parameters can be made without numerical integration of the system (Equations 25, 26, 27) formulated above. Let characteristic radius of cylindrical plasma channel be R_o at the end of laser pulse end with duration τ_L. Then characteristic velocity of plasma expansion is given by $u = R_o/\tau_L$ and characteristic pressure P_1 in plasma channel can be expressed as:

$$P_1 = \rho u^2 = \rho \frac{R_o^2}{\tau_L^2} \tag{28}$$

Using Equation (28) and the energy balance Equation (21) one can obtain the following approximate equation for R_o:

$$R_o = \left[\frac{(\gamma - 1)E_{abs}}{\pi \rho l} \right]^{1/4} \tau_L^{1/2} \tag{29}$$

and equation for P_1 can be obtained from Equations (28 and 29):

$$P_1 = \frac{1}{\tau_L} \left(\frac{\rho(\gamma - 1)E_{abs}}{\pi l} \right)^{1/2} \tag{30}$$

where E_{abs} is the laser energy absorbed during time interval τ_L, and l is the constant length of plasma-channel.

Pressure distribution in the acoustic wave propagating in a perpendicular direction to the axis of plasma-cavity is described by the following equation:[19]

$$P_1 = \frac{\rho R_o^4 l}{2\tau_L^2 d} \bullet \frac{L(t)}{Ln\dfrac{l}{R}} \tag{31}$$

where $\tau = \dfrac{t}{\tau_p} - \dfrac{d}{c_s \tau_L}$ is the normalized time, d is the distance measured from the plasma-channel axis to the observation point, R is the radius of plasma-channel in the moment t, R_o is the radius of plasma channel defined by Equation (29) and L(t) is the temporal profile of the laser pulse.

Maximum value of P_1 equals:

$$P_1 = \frac{\rho R_o^2}{2\tau_L d} \tag{32}$$

assuming $R_o^2 L(t) / Ln\dfrac{l}{R} \sim 1.$

10

Shock Waves from Spherical Plasma-Cavity

In some practical cases of focused laser irradiation or occurrence of self focusing effects, the characteristic diameter of the irradiation spot on the surface of the pigment epithelium (retina) is about 10 µm. The characteristic thickness of pigment epithelium layer, the main absorber of laser pulse energy, is about 5-10 µm. Therefore, in some short time after the end of the laser pulse, one may consider the shape of the plasma-cavity formed as a sphere. The expansion of the cavity produced by the thermally induced plasma leads to the formation and propagation of a spherical shock wave in ambient water of ocular tissue.

In this case laser-induced spherical plasma-cavity has initial radius $R_i \sim 0.001$ cm, initial temperature $T_i \sim (5\text{-}15) \cdot 10^3$ K, and pressure $P_i \sim 10^2 - 10^5$ bar.

Equations (21, 22, 23) are also valid in this case, where $V = 4/3\pi R^3$ and is the volume of plasma spherical-cavity with radius R.

Internal homogeneous pressure in the plasma-cavity is determined by the solution of the system of equations which describes the plasma expansion in water (tissue containing water) using the Kirkwood-Bethe model. This model accounts for the influence of liquid compressibility when the rate of plasma expansion is extremely high and approximately equals the speed of sound in water, C_s. The system has to be solved along with appropriate initial and boundary conditions.

$$\frac{du}{dt}\left(1 - \frac{u}{c'_s}\right) + \frac{3}{4}\frac{u^2}{R}\left(1 - \frac{1}{3}\frac{u}{c'_s}\right) = \left(1 + \frac{u}{c'_s}\right)\frac{H}{R} + \left(1 - \frac{u}{c'_s}\right)\frac{1}{c'_s}\frac{dH}{dt} \qquad (33)$$

$$H = \frac{c_s^2}{n-1}\left[\left(\frac{P+B}{A}\right)^{\frac{n-1}{n}} - 1\right] \qquad (34)$$

$$P = A\left(\frac{\rho'}{\rho}\right)^n - B \qquad (35)$$

This system of equations describes the shock wave amplitude in ambient water and can be integrated numerically if the expression of energy deposition E (t) is given.

Simple estimations of hydrodynamic parameters can be made without numerical integration of the system (Equations 33, 34, 35). Let the characteristic radius of plasma-cavity be R_o at the end of the laser pulse, τ_L. Then characteristic rate of plasma expansion is equal to $u = R_o / \tau_L$ and pressure P_1 in the cavity can be written as:

$$P_1 = \rho u^2 = \rho \frac{R_o^2}{\tau_L^2} \tag{36}$$

Using Equation (28) and the energy balance Equation (21) one can obtain the following approximate equation for R_o:

$$R_o = \left[\frac{3(\gamma - 1)}{4\pi\rho} E_{abs} \right]^{1/5} \tau_L^{2/5} \tag{37}$$

and equation for P_1 can be obtained from Equation (36 and 37):

$$P_1 = \rho^{\frac{3}{5}} \left[\frac{3(\gamma - 1)}{4\pi} \right]^{\frac{2}{5}} \frac{E_{abs}^{\frac{2}{5}}}{\tau_L^{6/5}} \tag{38}$$

For calculation of maximum amplitude of spherical shock wave the following equation can be employed:[21]

$$P = \frac{P_1 R_o}{2} g \exp\left(-\frac{t}{\theta} \right) \tag{39}$$

where parameter $\theta = 1 + 2/g$, $g = [M^{\frac{3}{2}} \sqrt{2Ln\left(\frac{d}{R_o}\right)}]^{-1}$ is the factor accounting for the nonlinear extinction of the shock wave, and $M = u/c_s = R_o/c_s\tau_L$ is the Mach number.

Equation (39) can be used in region placed far from the point of optical breakdown. In addition the following condition must be fulfilled: $Ln\frac{d}{R_o} \geq \frac{1}{4M^3}$.

On the basis of Equation (39) we can evaluate the shock wave energy and its relation to the laser energy absorbed by plasma, which characterizes the coefficient of laser energy transformation into the shock wave (acoustic) energy:

$$\eta = \frac{3}{2}(\gamma - 1)\left(M \bullet \ln\frac{d}{R_o} \right)^{\frac{1}{2}} \tag{40}$$

η has maximum value of about 20-30 %.

Pressure amplitude, P_{max}, on the front of a spherical shock wave can be estimated by interpolation of the following equation:

$$\frac{P_{max}}{A} = \frac{8}{25}\frac{n}{n+1}\left\{0.611\left[\left(1+0.16\frac{nA}{E}R_*^3\right)^{\frac{5}{18}}-1\right]\right\}^{-1} \qquad (41)$$

where R_* [cm] is the radius of shock wave front, $n = 7$, $A = 3001$ bar, P_{max} [bar] is the maximal pressure in the shock front, and E [J] is the absorbed laser energy.

The following condition must be satisfied (strong shock wave): $P_{max} > 0.02\,P_o$ where P_o is the pressure value in water obtained using the equation of state for water from the system of Equations (33, 34, 35).[22]

This interpolation-equation (41) is transformed to the strong explosion solution near the breakdown point and precisely describes the extinction of shock wave at long distances of the observation point. Hydrodynamic and acoustical processes during laser breakdown of water and other liquids were experimentally investigated in numerous studies.[23-27]

Pressure Wave Generation upon Thermal Explosion of Melanosome

Evaporation of Water and Expansion of Vapor Bubble Initiated by Laser Heating of Melanosome

Let a spherical melanosome of radius $r_o \mathring{A} 1\ \mu m$ be situated in ocular tissue containing water and irradiated with a focused short laser pulse. Because of microscopic dimensions of the melanosome, heat exchange between adjacent water layers has to be considered simultaneously with the process of laser energy absorption by the melanosome. Water contained tissue has thermophysical parameters similar to that of water, and therefore, for simplicity we may consider a melanosome placed in water. Let the melanosome and the adjacent water layer be rapidly superheated to a temperature T^* higher than water evaporation temperature $T_b = 100°\ C = 373°\ K$ as a result of a short laser pulse irradiation under the atmospheric pressure. In this case the water surrounding the melanosome can be transferred into the metastable state and undergo explosive vaporization. Phase transition (vapor generation) will occur only in the water layer that surrounds the melanosome. The thickness of this layer, δ, can be calculated using the simple heat diffusion equation:[28]

$$\delta = \sqrt{4\chi\tau_L} - r_0 \qquad (42)$$

It is experimentally established that the maximum value temperature T^* of intense homogeneous nucleation (explosive evaporation) can reach is $T^*=578-593$ K under short-pulse laser irradiation.[29,30] Practically, the process of explosive evaporation can be

initiated at the temperature value lying in the interval $640 > T^* > 373$ K in various experimental situations. The higher the temperature of superheating, the shorter the time-delay between laser energy deposition and the moment of thermal explosion. The rate of vapor bubble formation, $J(T)$, expressed in [1/s cm^3] is given by the Döring-Volmer equation modified by Stranski:

$$J(T) = n \left[\frac{6\sigma}{\pi m \left(2 + \dfrac{P'}{P''} \right)} \right]^{\frac{1}{2}} \exp\left(-\frac{W_c(T)}{kT} \right) \partial(\theta) \qquad (43)$$

where n is the number of molecules per unit volume of superheated tissue, $\sigma(T)$ is the surface tension of the superheated liquid medium at the temperature T^*, m is the mass of the superheated liquid molecule, P' is the external pressure in tissue (or liquid), P'' is the saturation vapor pressure in the bubble at $T=T^*$, $W_c(T)$ is the work of formation of the critical size vapor bubble, $\partial(\theta)<1$ is the coefficient of the angle of contact, θ, that account for the decrease of $W_c(T)$ because of the presence of the non-moistening surface of melanosome, and k is the Boltsman constant.

$$W_c(T) = \frac{16\pi\sigma^3}{3(P''-P')^2} \qquad (44)$$

The average delay time between the moment of laser energy deposition and the moment of critical size vapor bubble formation on the surface of superheated melanosome can be calculated as:

$$\tau_b = 1/ J V \qquad (45)$$

We assume that the explosive evaporation of adjacent water layer occurs instantly, and the initial vapor layer around the melanosome also forms instantly at the moment, τ_{10}, defined as:

$$\tau_{10} = \tau_0 + \Delta\tau_e \qquad (46)$$

where τ_0 is the moment when the melanosome surface reaches the temperature, T^*, and $\Delta\tau_e$ is the duration of explosion.

After instantaneous explosive vaporization, the spherical vapor bubble will be formed with initial radius $r_{10} = r_0 + \delta$, where δ is the thickness of water layer superheated due to heat diffusion prior to explosion ($\delta = 1\text{-}5$ µm), and initial vapor temperature T_{10}, pressure P_{10} and density ρ_{10}. In this case, the pressure P_{10} and density ρ_{10} of the vapor equal correspondingly to the pressure, P_{1S} and density, ρ_{1S} of the saturated water vapor at

14

the temperature T_{10}. The mass M_{10} of the vapor bubble formed around the spherical melanosome and its initial outer radius r_{10} can be found from the system of three equations: mass conservation law (47), energy conservation law (48), and the equation of the saturated vapor state (49).[31]

$$V_{20}\rho_2 = M_{10} = V_{10}\rho_{1S}(T_{10}) \tag{47}$$

$$4\pi\rho_2 \int_{r_0}^{r_*} r^2 C_2 T(r)dr = (P_{10} - P_0)(V_{10} - V_{20}) + 4\pi r_{10}^2 \sigma + M_{10}(E_{10} + Q_v) \tag{48}$$

$$P_{10} = P_{1S} = R_g \rho_{1S}(T_{10})T_{10} \tag{49}$$

where $r^*=r$ at $T=T^*$ is the radius of the volume in tissue where temperature, T, has reached the value of T^*, volume $V_{10} = \frac{4}{3}\pi(r_{10}^3 - r_0^3)$ is the initial volume of vapor bubble produced from the water heated to the temperature T_{10} (vapor pressure equal that of saturation at T_{10}), and $V_{20} = \frac{4}{3}\pi(r_{20}^3 - r_0^3)$ is the total volume of water transformed into the vapor state (vapor bubble produced from the water layer with outer radius, r_{20}); C_1, C_2 [J/g °K] are respectively the heat capacity of vapor and water, R_g is the gas constant, σ[J/cm^2] is the surface tension coefficient, Q_v is the specific heat (energy) of vaporization per unit mass, ρ_1 and ρ_2 are the densities of vapor and water respectively, P_1 is the vapor pressure, P_0 is the initial external pressure in water (tissue), distribution $T(r)$ is determined from the solution of the heat conduction equation, which describes heat exchange between melanosome and adjacent water. Solution of the system of Equations (47, 48, 49) with the known value of T_{10} yields the initial parameters r_{10}, ρ_{10}, P_{10}, M_{10} which can be used as initial conditions in consideration of the vapor bubble dynamics in aqueous ocular medium.

Let us assume a spherical vapor bubble expands according to the law $R(t)$ with the rate dR/dt lower than the speed of sound in water, C_s. Let us also assume that water is absolutely incompressible. During adiabatic expansion the vapor pressure in the spherical bubble is described by the following equation:

$$P_1 = \rho_{10}\left(\frac{r_{10}}{R}\right)^{3\gamma} \tag{50}$$

where γ is the adiabatic exponent factor for water vapor. Raleigh equation, describing the bubble expansion process can be given as:

$$R\frac{d^2R}{dt} + \frac{3}{2}\frac{dR^2}{dt} = \frac{1}{\rho}\left[\rho_{10}\left(\frac{r_{10}}{R}\right)^{3\gamma} - P_0\right] \tag{51}$$

Equation (51) can be integrated (solved) only using numerical methods with initial conditions. The pressure in compression wave originating by expanding bubble is described by the following equation:[19]

$$P = P_0 + \frac{R}{r}\left[P_{10}\left(\frac{r_{10}}{R(t')}\right)^{3\gamma} - P_0 + \frac{1}{2}\rho_0\left(\frac{dR(t')}{dt}\right)^2\left(1 - \frac{R^3(t')}{r^3}\right)\right] \qquad (52)$$

where t' = t - r/C$_s$. If R(t) is known from Equation (52) one can obtain the pressure distribution that consists of the short compression pulse generated during initial stage of expansion under P > P$_0$ followed by the longer pulse of rarefaction.

Accounting for compressibility of water, the pressure distribution in wave zone is determined by the linear acoustic solution:

$$P = P + \rho_0\frac{d^2V(t')}{4\pi r} \qquad (53)$$

where $V = 4/3\pi R^3$, r is the radius to the point of observation, t'= t - r/C$_s$. Simple estimation of some parameters of compression wave gives the velocity of bubble expansion $\frac{dR}{dt} \sim \sqrt{\frac{P_{10}}{\rho_0}}$, pressure in compression pulse $P \sim \frac{P_{10}r_{10}}{r}$, duration of compression pulse, $\tau \sim r_{10}\sqrt{\frac{\rho_0}{P_{10}}}$, energy of compression pulse $W \sim 4\pi r^2\frac{P^2\tau^2}{\rho_0 C_S}$, a fraction of initial heat energy of vapor, converted to energy of compression wave $Q_v \sim 3(\gamma - 1)\frac{r_{10}}{C_s\tau}$.

Pressure distribution in an acoustic wave during initial stage of compression wave is described by the following equation:[19]

$$P = \rho_0\frac{R_0^5}{\tau_L^2 r}\frac{f(t')}{R^2} \qquad (54)$$

where R$_o$ is determined by Equation (37), $t' = \frac{1}{\tau_L}(t - \frac{r}{C_S})$, L(t') is determined by the temporal profile of the laser pulse, see Equation (1). Stress generation upon interaction of a short laser pulse with spherical particles placed in liquid and vapor bubble growth on particles was experimentally investigated by Golubnichiy et al.[32]

In the case when temperature T* of explosive evaporation is only slightly higher compared with the threshold temperature of thermal explosion, dR/dt<C$_S$, equations presented above can be used to describe the linear acoustic wave generation. For

example, heating a melanosome to $T_{10} = 120°$ C (393 K) causes a pressure-rise of about 2.2 bar. An acoustic wave with an amplitude of about 2-3 bar can not cause any significant damage to adjacent ocular tissues.

Thickness of Compressed Tissue in the Shock Front

To determine the thickness d of the compressed tissue or water layer near the shock front, let us calculate the work (dW) done in compressing a volume element dV:

$$dW = PdV \qquad (55)$$

Substituting the coefficient of isothermal compressibility of tissue, γ, defined according to Equations (15 and 16) as:

$$\gamma = \frac{1}{V}\frac{dV}{dP} \qquad (56)$$

in Equation (55) and integrating, one can obtain:

$$W = \frac{1}{2}V\gamma P^2 \qquad (57)$$

For a spherical wave of radius R,

$$W = 2\pi R^2 \delta \gamma P^2 \qquad (58)$$

therefore,

$$\delta = \frac{W}{2\pi R^2 \gamma P^2} \qquad (59)$$

STRESS WAVE PROPAGATION

Stress Relaxation

Consideration given in Stress Transients in the Near Zone is strictly valid only in the case when the process of heating is much faster than the process of medium expansion. It is said that "stress is confined" under such irradiation conditions. If stress is confined in a medium, the initial magnitude of the pressure in the heated volume may be expressed with Equation (19). In other words, the Equation (19) describes the initial, instantly generated

17

pressure amplitude prior to the stress wave propagation through the optical zone. It means that in this case the laser pulse duration, τ_L, has to be much shorter as compared with the time it takes for the stress wave to propagate the distance equal to the effective penetration depth of light, l_{eff}. This condition of laser irradiation is referred to as "confined stress" condition.

$$\tau_{sr} = l_{eff} / C_s \gg \tau_L \tag{60}$$

The stress relaxation time, τ_{sr}, is defined as the time it takes for the sound to propagate through the thickness of the irradiated volume. Taking into account that absorption in melanin granules dominates, we may neglect scattering in the retinal pigmented epithelium (RPE) and the process of heat diffusion can also, in principle, cause some decrease of the thermoelastic stress amplitude. However, the heat diffusion time, τ_{hd}, in the vast majority of media (and particularly in ocular tissues) is much longer than the stress relaxation time, τ_{sr}. Therefore, practically in all cases we can neglect the decrease of pressure in the irradiated tissue due to heat diffusion as compared with the stress relaxation.

When the stress relaxation parameter, $\mu_a C_s \tau_L$, is not very small, the measured pressure is lower than that calculated by the Equation (63). Stress relaxation changes both the amplitude and the shape of the pressure distribution generated in the sample. The actual acoustic pulse profile formed by the laser pulse profile, L(t), can be calculated as the convolution of the instant spatial distribution of the thermoelastic sources moving into the media and temporal intensity envelope of deposited laser energy:

$$P(t) = \Gamma C_S \mu_a I_0 \int_{-\infty}^{+\infty} L(t) \exp(-\mu_a C_s |t - \tau_L|) \, dt \tag{61}$$

Temporal profiles of the Nd:YAG laser pulses used in our experiments can be described by the Gaussian distribution:

$$L(t) = (\pi)^{-1/2} \cdot \exp[(-2t / \tau_L)^2] \tag{62}$$

where τ_L is the full pulse duration at 1/e of amplitude.

Equation (61) does not have a simple analytical solution and must be numerically calculated. In a more simple case of a rectangular temporal profile of a laser pulse, Equation (61) can be given by:

$$P(t) = \Gamma c_s \mu_a I_0 \frac{(1 - \exp(-\tau_L / \tau_{sr}))}{(\tau_L / \tau_{sr})} \tag{63}$$

When the laser pulse is long enough in comparison with $1/(\mu_a C_s)$, the profile of acoustic signal reproduces the derivative of the laser pulse shape.

$$P(t) = \Gamma \, \mu_a \, I_0 \, L(t) \, \tau_L \qquad (64)$$

In the case of finite duration of laser pulses, the stress relaxation may affect only the amplitude of the generated acoustic signal if τ_p is shorter than τ_{sr}. The amplitude of the acoustic signal drops down while its exponential wings change negligibly, because higher acoustic frequencies dissipate faster than low frequencies. Practically, the latter is valid when the confined-stress-parameter, $\mu_{eff} C_s \tau_L < 1$.

Figure 2 depicts the ratio of the real stress amplitude, P, that may be measured or calculated from Equation (63), and theoretically maximal amplitude, P_{max}, calculated from Equation (64) as a function of the stress relaxation parameter, $\mu_{eff} C_s \tau_L$.
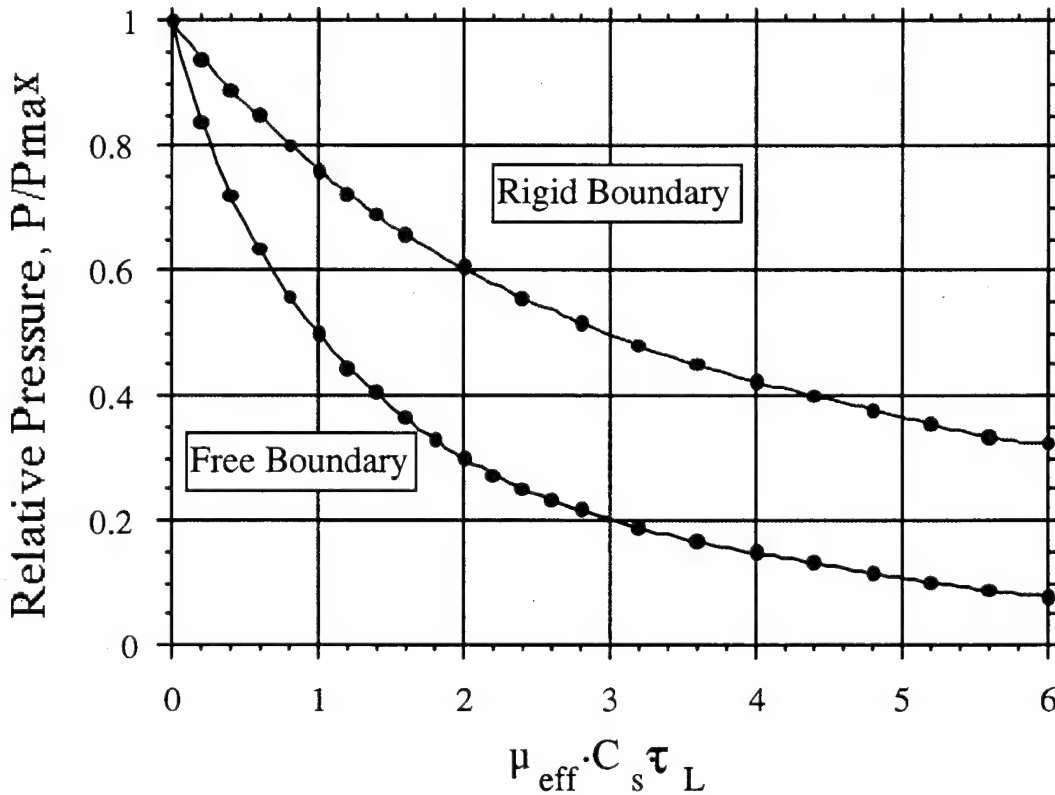
FIGURE 2. Theoretically calculated relative stress amplitude as a function of the stress relaxation parameter, $\mu_a C_s \tau_L$, in two cases of (a) "free" tissue boundary, (b) "rigid" tissue boundary.

There are two limit cases that can be considered for the boundary conditions between tissue and surrounding medium: (1) - "free" surface, when the acoustic impedance of tissue is much greater than the product of density, ρ, and the speed of sound for the medium (for example, air) above it, and (2) - "rigid" boundary, when the acoustic

impedance of tissue under heating is less as compared with that of any more dense medium (for example, detector plate) beneath it.

The stress relaxation in these two cases as a function of stress relaxation parameter has different behavior. In case of the "free" boundary, transient stress profile, $S_f(t)$, can be expressed as a derivative of the stress profile in the case of "rigid" boundary, $S_r(t)$.

$$S_f(t) = \frac{1}{\mu_a C_S} \bullet \frac{dS_r(t)}{dt} \qquad (65)$$

Therefore, stress amplitude in the case of a free boundary decreases faster with the increase of laser pulse duration as compared with the case of "rigid" tissue boundary.

Wide laser beams incident on the eye can generate plane acoustic waves in the absorbing tissue of the RPE layer. However, focused laser beams of very small diameter may generate spherical or cylindrical acoustic waves. In cases where a stress wave is caused by the optical breakdown, the shape of an acoustic wave front will be presented by a plasma jet in the caustic of the focused laser beam. The stress wave propagation should be considered in the cylindrical geometry, where pressure magnitude decreases in proportion to $1/\sqrt{r}$ with the increase of distance, r, from the source (see section titled Cylindrical Plasma-Cavity.). In cases where a laser beam is absorbed in a single melanosome that has a nearly spherical shape with diameter of about 1.5 µm, generated acoustic waves will be represented by an expanding sphere, where pressure magnitude decreases as 1/r, where r is the sphere radius (see section titled Spherical Plasma-Cavity).

Acoustic Wave Reflection

At the onset of heat generation in the irradiated volume, a pressure wave propagates along the laser beam axis in the sample in two directions (one opposite to the other: into the sample and toward the sample surface). The value of the pressure amplitude propagating at the speed of sound, C_s, in each direction is equal to half of the initial amplitude of thermoelastic stress. Acoustic waves propagating toward the tissue surface may be reflected. The value of reflectance, R_{ac}, and its sign are defined by the mismatch of acoustic impedance, ρC_s, at the boundary of tissue and surrounding medium.

The coefficient of acoustic wave reflection, R_{ac}, is equal to the ratio of pressure amplitudes of the incident, P_o, and reflected, P_{ref}, waves and can be calculated using the ratio of acoustic impedances as:

$$R_{ac} = \frac{P_{ref}}{P_o} = \frac{(1 - \rho C_s / \rho' C'_s)}{(1 + \rho C_s / \rho' C'_s)} \qquad (66)$$

20

The Equation (66) indicates that in the case of "free" tissue boundary ($\rho C_s \gg \rho'C'_s$), the reflected stress wave changes its sign and becomes a negative (tensile) wave. Therefore, the acoustic wave propagating into the tissue from the irradiated surface manifests itself as a "butterfly" with symmetric exponential wings formed by the axial light distribution (see Figure 3). In the case of the "rigid" tissue boundary ($\rho C_s \ll \rho'C'_s$) acoustic reflectance, R_{ac}, has a positive sign, and the transmitted acoustic wave propagates into the more dense medium without sign change.
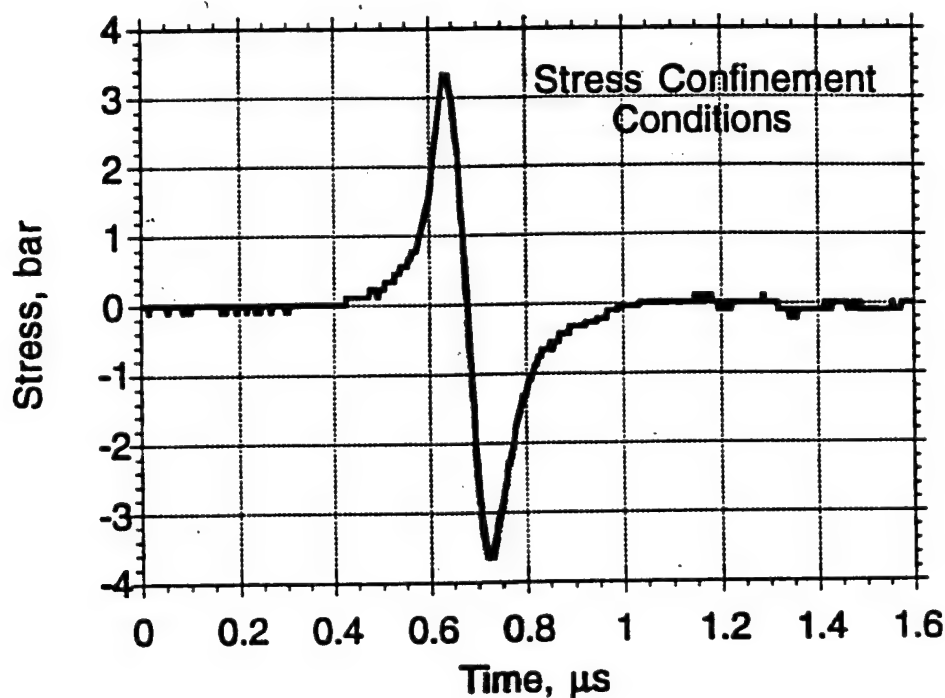
FIGURE 3. Laser induced transient stress in cornea irradiated at 266 nm in air under confined stress conditions.

Acoustic Wave Transmission

As long as the sample under study is separated from the piezoelectric transducer by an acoustic conductor slab, it is essential to understand the process of stress transmission through a boundary between two media. Let us calculate the transmitted pressure amplitude in the case when the laser-induced plane acoustic wave propagates perpendicularly to the surface of an interface.

The transmitted intensity of the acoustic wave can be expressed as:

21

$$\frac{I_t}{I_i} = \frac{4\rho_i C_{s_i} \rho_t C_{s_t}}{(\rho_i C_{s_i} + \rho_t C_{s_t})^2} \tag{67}$$

where ultrasound velocities C_{s_i} and C_{s_t} and densities ρ_i and ρ_t are associated with the incident and transmitted waves, respectively. The acoustic wave intensity is proportional to the pressure amplitude squared:

$$I = P^2 / \rho \, C_S \tag{68}$$

Therefore, transmitted pressure may be given by:

$$T = \frac{P_t}{P_i} = \sqrt{\left(\frac{I_t \rho_t C_{s_t}}{I_i \rho_i C_{s_i}}\right)} = \frac{2\rho_t C_{s_t}}{(\rho_i C_{s_i} + \rho_t C_{s_i})} \tag{69}$$

There is an important and maybe at first unexpected conclusion, based on Equation (69): the pressure in the transmitted acoustic wave, P_t, can be higher than that incident upon the boundary. The value of the pressure transmittance, T, equals **2** when the acoustic impedance of the i-medium is much lower as compared to the acoustic impedance of the t-medium. In contrast, when stress propagates from melanosome into an aqueous environment, the transmitted pressure will be 1.13 times lower than that generated in melanin granule.

Note:
($\rho_{water} C_{S_{water}}$=1.0[g/cc]•1.49x10⁵ [cm/s]),
($\rho_{tissue} C_{s_{tissue}}$=1.1[g/cc]•1.77x10⁵ [cm/s]).

Alteration of an Acoustic Wave upon Propagation

Spatial and temporal profiles of a laser-induced stress transient can be changed during propagation in ocular tissue. The measured signal can be altered by the medium due to the diffraction of the acoustic wave, D, as well as its attenuation, Λ, stress relaxation, R, and transmittance through interfaces, T, and by the tissue nonlinear acoustic properties. Acoustic nonlinearity can dramatically change the profile of a high-amplitude stress wave during its propagation in tissue causing formation of a shock front with dramatic pressure gradient (see section titled Formation of a Shock Wave from High-Amplitude Acoustic Waves).

Thus, the profile of an acoustic signal is determined by optical and acoustical properties of a medium as well as by the laser irradiation parameters, such as pulse duration, beam diameter, and energy fluence. The measured acoustic signal can be

generally described by the following equation that includes phenomena to be considered in the following sections.

$$P(z) = (\Gamma/2) \cdot \mu_a \cdot \Phi_0 \cdot R(z) \cdot T \cdot D(z) \cdot \Lambda(z) \cdot N \tag{70}$$

Acoustic Wave Diffraction

The acoustic diffraction plays the most important role in the dissipation of thermoelastic waves. The reason for diffraction is the finite size of the area of stress-generation, which causes a gradual transformation of a plane wave into a spherical wave. The initial consequence of diffraction is the increase of effective area of the acoustic wave, which leads to a decrease of the pressure amplitude and change of the acoustic signal profile.

The effective diameter of the acoustic wave, w_{aw}, at a depth, z, within medium is expressed as:

$$w_{aw} = w_L \sqrt{1 + \left(\frac{z}{z_D}\right)^2} \tag{71}$$

where w_L is the laser beam diameter at the tissue surface, and z_D is the effective depth of diffraction.

z_D is defined as:

$$z_D = \pi n w_{aw} = \frac{\pi f_s w_L^2}{C_s} \tag{72}$$

where f_s - acoustic wave frequency, w_L - laser beam diameter, C_s - velocity of acoustic wave propagation, $n = w_L / \lambda$ is number of acoustic wavelengths, and $\lambda = C_s/f_s$ which fits into the diameter of acoustic wave at the surface of the irradiated sample.

The acoustic wave frequency is defined by the optical properties of irradiated medium and the speed of sound in this medium:

$$f_S = \mu_{eff} \cdot C_s \tag{73}$$

Thus, the diffraction depth can be estimated as:

$$z_D = \pi \cdot \mu_{eff} \cdot w_L^2 \tag{74}$$

23

Substituting Equation (74) in Equation (71) we get the equation for the effective area of a plane acoustic wave as a function of sample thickness, optical attenuation coefficient and laser beam diameter:

$$w_{aw} = w_L \sqrt{1 + (Z / \pi \mu_{eff} w_L^2)^2} \qquad (75)$$

Figure 4 shows effective acoustic beam diameter with respect to initial laser beam width for two acoustic frequencies, 0.55 MHz and 75 MHz. The diffraction process is efficient for low acoustic frequencies and small beam diameters. The integration of all thermoelastic sources of spherical acoustic waves to form the plane wave propagating toward the acoustic transducer occurs at the distance, z, that is not less than $5/\mu_{eff}$. Therefore, an accurate measurement of low light attenuation requires absolutely larger thicknesses of the sample as compared to the case for high attenuation coefficient, μ_{eff}. Figure 4 demonstrated that in case of low absorbing medium, the ratio of z/z_D can be substantial and diffraction has to be taken into account. In contrast, high acoustic frequencies are not affected by diffraction even when initial diameter is as low as 1 mm.
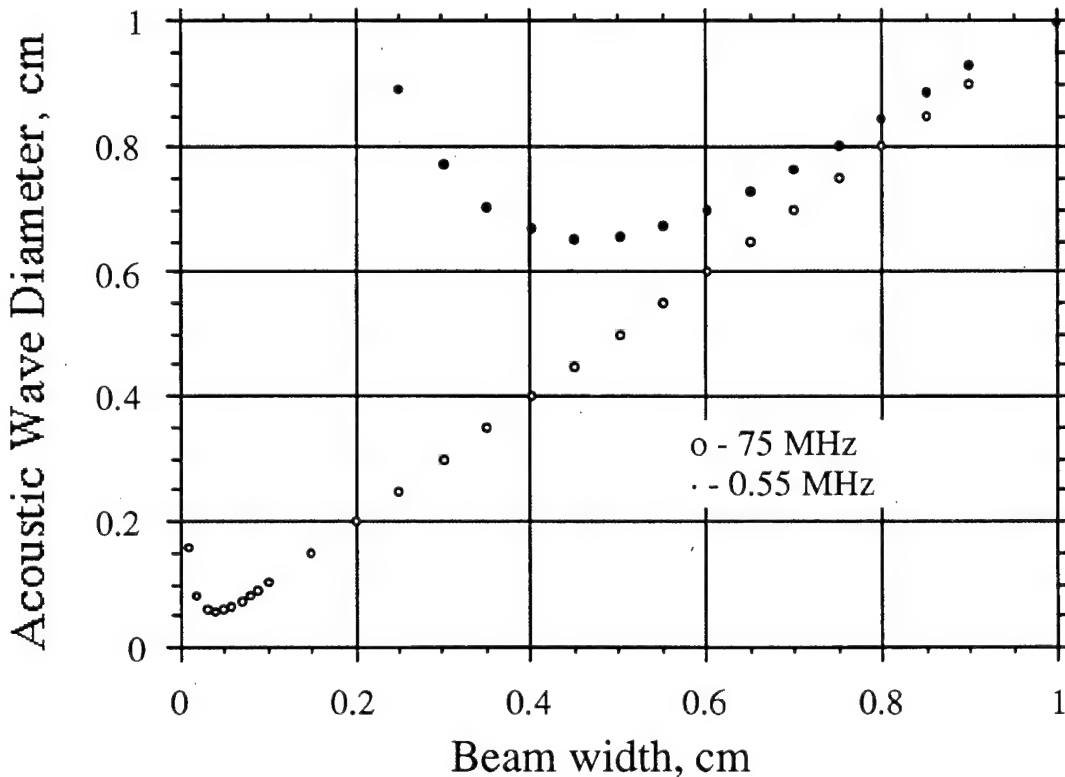

FIGURE 4. Demonstration of acoustic wave diffraction effect. The effective diameter of acoustic wave is plotted as a function of laser beam diameter according to Equation (77) for low (0.55 MHz) and high (75 MHz) acoustic frequencies.

24

The acoustic wave diffraction can be taken into account as the D-factor proportional to the ratio of laser beam area, A_L (or effective acoustic wave area at the sample surface), and acoustic wave area, A_{aw}, in the plane of interest on the z-axis given by:

$$A_{aw} = \pi w_{aw}^2 / 4 = (\pi / 4)(1 + (z/z_D)^2) w_L^2 \tag{76}$$

and ratio of acoustic wave areas at the sample and transducer surfaces is expressed by:

$$D = \frac{A_L}{A_{aw}} = \frac{1}{\left(1 + (z/z_D)^2\right)} = \frac{1}{\left(1 + \left(z \dfrac{z}{\pi \mu_{eff} w_L^2}\right)\right)} \tag{77}$$

Figure 5 depicts the diffraction parameter for highly absorbing and low absorbing solutions (i.e., high and low acoustic frequencies). Theoretical curves of the diffraction parameter, D, calculated according to the Equation (77) agree well with the experimental measurements of relative pressure magnitude as a function of laser beam diameter.

Acoustic Wave Attenuation

The absorption and scattering of the acoustic wave energy causes an alteration of both the amplitude and exponential profile of the initial z-axial distribution of initial laser-induced stress. As far as we are interested in optical properties of media, it is convenient to combine acoustic absorption and scattering in one attenuation coefficient, α, equal to the sum of acoustic absorption and scattering coefficients.

$$P(z) = P_O(z) \cdot \Lambda(z) = P_O(z) \exp(-\alpha(d-z)) \tag{78}$$

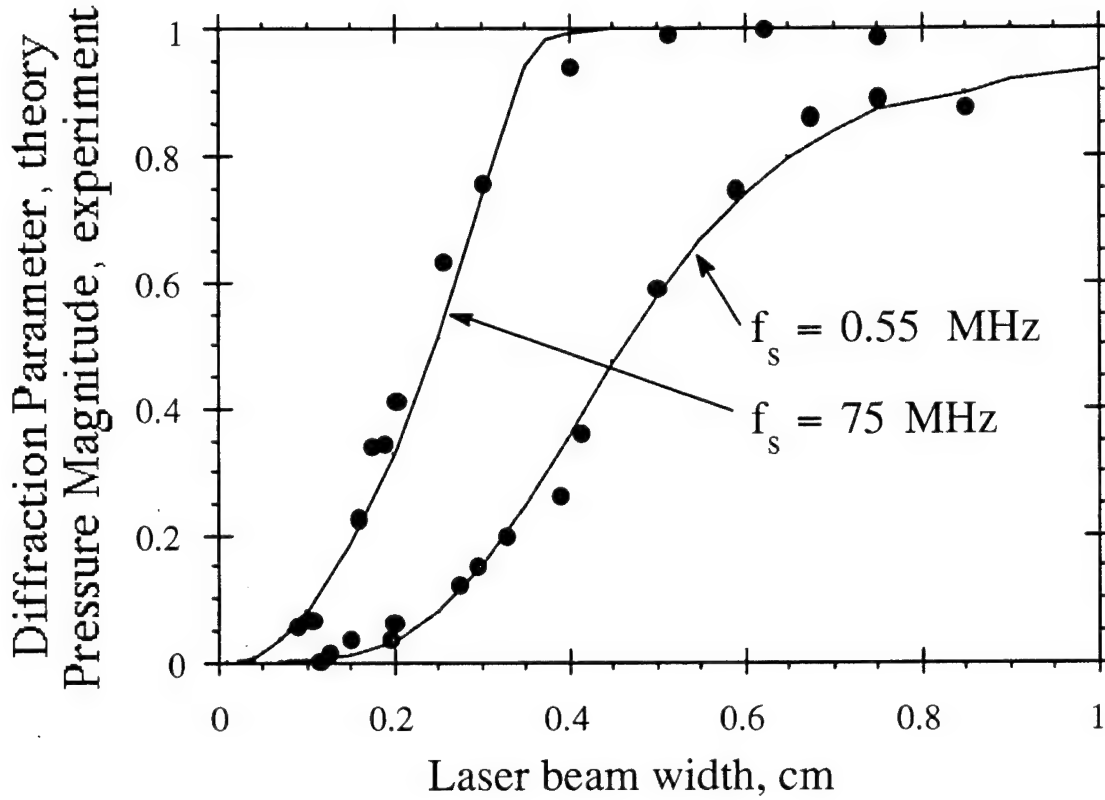where $P_O(z)$ is initial z-axial pressure distribution.

FIGURE 5. Diffraction parameter shown as a function of laser beam diameter in the case of low and high frequencies of acoustic wave. Experimental points are superimposed with theoretical curves, calculated based on Equations (77 and 78).

Equation (78) takes into account that during propagation toward the detector, subsurface stress will be attenuated stronger as compared to the stress generated in depth of tissue sample. Ultrasonic attenuation and other acoustic properties of biological tissues have been extensively studied after the invention of ultrasonic imaging.[14] Acoustic attenuation rises linearly with ultrasonic frequency for the vast majority of tissues. Acoustic attenuation coefficient in soft tissues is negligibly low in the frequency range of several hundred kHz that corresponds to optical attenuation, μ_{eff}, about 1-3 cm^{-1}. When acoustic frequency reaches 1 MHz, the value of α increases to (0.01 - 0.05) cm^{-1}. For high ultrasonic frequencies, above 10 MHz attenuation of acoustic waves becomes pronounced, (0.1-1.0) cm^{-1}. In contrast to biological tissues, attenuation coefficient for acoustic waves in liquids has stronger frequency dispersion and proportional to f_s^2 in the range (1-100) MHz. The attenuation of acoustic waves in pure water can be calculated as $\alpha \ [cm^{-1}] = 2.5 \times 10^{-16} \cdot f_s^2 \ [Hz^2]$.

Formation of a Shock Wave from High-Amplitude Acoustic Waves

The profile of high amplitude acoustic waves can be altered upon propagation in biological tissues. The major consequence of nonlinear propagation of high amplitude

acoustic waves in media is formation of shock waves (so called "relatively weak shock waves"). Shock front can be formed after the propagation at the distance L, that is dependent on the pressure amplitude, P_o, and the parameter of acoustic nonlinearity, ε, of the given tissue (ε=3.5 - 6.0 for soft tissues).

$$\varepsilon = 1 + \frac{\rho}{2C_s^2} \frac{\partial C_s^2}{\partial \rho} \tag{79}$$

The distance of shock wave formation can be expressed the following ways:

$$L_{sh} = \frac{\lambda_{ac}}{2\pi\varepsilon M} = \frac{l\rho C_s^2}{\varepsilon P_o} = \frac{\rho C_s^3}{2\pi\varepsilon P_o f_{ac}} \tag{80}$$

where $M = v_p / C_s$ is the Mach number, the ratio of particles velocity in the acoustic wave and the speed of sound in tissue, l is the length of the acoustic pulse in the direction of the laser beam, maximal pressure amplitude can be estimated using Equation (18).

Practical examples to be used for simple estimations of laser interactions with ocular tissue.

(1) Nanosecond laser pulse at 2.1-μm wavelength produces acoustic transients in a RPE layer with amplitude of P_o=1 bar and frequency of 100 MHz. Taking ρ=1.1 g/cm^3, $C_S = 1.6 \cdot 10^5$ cm/s, ε=5.0 one can get the distance of the shock wave formation L=0.11 mm.

(2) It was experimentally observed that a stress transient with acoustic pressure amplitude of approximately 20 kbar and pulse duration of about 0.75 ns can be generated upon irradiation of water by a short laser pulse with $\tau_L = 80$ ps, 2.94-nm wavelength, laser pulse energy of 60 mJ, and intensity of 10 GW/cm^2.[6] Estimation of P_o using the Equation (18) and value for Γ=0.3 gives the value P_o = 30 kbar in accordance with experimental value P_o = 20 kbar. The empirical "equation of state" for water is:

$$P = A\left(\frac{\rho'}{\rho}\right)^n - B \tag{81}$$

where A=3.001 kbar, B=3.0 kbar, n=7, and ρ'=1.3ρ is water density at 20 kbar pressure.[15] From the simple system of equations for shock wave

$$P = \rho v_p C_{sh} \tag{82}$$

$$\rho' = r \, (C_{sh}/C_{sh}-v_p) \tag{83}$$

one can calculate that the shock wave velocity $C_{sh} = 2.9 \cdot 10^5$ cm/s is about twice higher compared with the speed of sound in water, and the velocity of particles in liquid, $v_p = 6.9 \cdot 10^4$ cm/s is about twice lower compared with the speed of sound, C_s.

Intensity of sound energy is equal to:

$$I_s = \rho C_{sh} v_p^2 = 1.85 \cdot 10^8 \;\; W / cm^2 \tag{84}$$

and efficacy of conversion of optical energy into the mechanical stress energy is

$$\eta = \frac{I_s \tau_s}{I_o \tau_L} = 5.8\% \tag{85}$$

(3) Let us discuss the case of free surface of liquid irradiated with a short laser pulse. The following one-dimensional equation can be drawn for the plane (flat disk) geometry of irradiation:[7]

$$P = \frac{\beta I_o}{\mu_a C_s t_{max}} \cdot 3(\Theta'^2 - \Theta'^3) \exp 3(1 - \Theta'), \;\; for \;\; \Theta' \geq 0 \tag{86}$$

where t_m is the rise time of the laser pulse at maximum value of intensity, $\Theta' = \dfrac{t - z/C_s}{t_m}$,

$a \gg 1/\mu_{eff}$

Temporal profile, L, of the laser pulse can be approximated by a simple equation:

$$L(\Theta) = \Theta^3 \exp[3(1 - \Theta)] \;\; for \;\; \Theta \geq 0 \tag{87}$$

The Equation (86) represents a bipolar pressure pulse with a positive *extremum* at $\Theta = 0.42$ with the stress peak amplitude:

$$P_{max}(\Theta' = 0.42) \approx 0.09 \frac{\beta I_0}{\mu_a C_p t_{max}} e^3 \tag{88}$$

followed by a smaller negative *extremum* at $\Theta' = 1.58$ with an amplitude:

28

$$P_{max}(\Theta' = 1.58) \approx -0.04 \frac{\beta I_0}{\mu_a C_p t_m} e^3 \tag{89}$$

Therefore P_{max} is inversely proportional to μ_a for extremely strongly absorbing media. These equations are in good agreement with experimental data. For example, in Cleary and Hamrick[9] and Cleary[10] laser-induced stress transients in the mammalian eye resulted from the absorption of Q-switched ruby laser pulses with duration of about 100 ns and spot diameter of 750 µm. Stress amplitudes were measured at the level of 100-1000 bar in the immediate vicinity of the site of absorption on the rabbit retina. The minimum pressure amplitudes encountered in the energy - density region associated with minimal threshold lesions are of the order of 10-30 bar.

The general system of equations that describes a profile of a pressure wave generated upon impact or expansion of a medium with velocity, v_m is given below.

Continuity equation:

$$\frac{\partial \rho}{\partial t} + \frac{\partial}{\partial z}(\rho v_m) = 0 \tag{90}$$

Conservation of impulse:

$$\frac{\partial}{\partial t}(\rho v_m) + \frac{\partial}{\partial z}\left(P + \rho v_m^2 - \frac{4}{3}\eta \frac{\partial v_m}{\partial z}\right) = 0 \tag{91}$$

Conservation of energy:

$$\frac{\partial}{\partial t}\left(\rho \varepsilon + \frac{\rho v_m^2}{2}\right) + \frac{\partial}{\partial z}[\rho v_m\left(\varepsilon + \frac{v_m^2}{2}\right) + \rho v_m - \frac{4}{3}\eta v_m \frac{\partial v_m}{\partial z} - \kappa \frac{\partial T}{\partial z} = 0 \tag{92}$$

where $\varepsilon = 4.2$ kJ/g K is specific heat of water evaporation, $\kappa = 0.56$ W/m g is the thermal conductivity of water, and η is the coefficient of dynamic viscosity.

When speed of ultrasonic wave as a function of pressure amplitude is known, one can compute the system (Equations 94, 95, 96) to find out whether initial stress transient will be converted into a shock upon propagation or dissipation will dominate.

Heating of Tissue by a Shock Wave

Although the laser radiation does not penetrate into the "cold" zone (heat diffusion is absent for the nanosecond pulses), the shock wave does propagate far beyond the point of generation. One of the side effects of the shock wave to adjacent tissue layers can be the heating of tissue due to the adiabatic compression by a shock wave[33] where u_s is the mass velocity (particles velocity) in the shock wave.

$$\Delta T = \frac{C_s T \beta u_s}{C_p} \tag{93}$$

For example, a 20 kbar shock wave alters intermolecular distance in tissue by approximately 10% and can heat the adjacent layers to $\Delta T \approx 57^\circ$ C.

REFERENCES

1. Ready J. "Effects of high-power laser radiation". Academic Press. New York, 1971.

2. Lyamshev L., Sedov L. Optical generation of sound in liquid. Heat mechanism. Review. *Sov. Acoustic Journal* 1981; **27**(1): 5-29 (in Russian).

3. Lyamshev L. "Laser thermo-optical excitation of sound". Moscow. Nauka, 1989.

4. Egerev SV, Lyamshev L, Puchenkov O. Laser transient pulse diagnostics of condensed matter. *Sov. Physiscs Uspekhi* (U.Ph.N.) 1990; **160**(9): 111-154.

5. Berthelot Y, Busch-Vishniac J. Laser-induced thermo-acoustic radiation. *J. Acoust. Soc. Am.* 1985; **78**(6): 2074-2082.

6. Vodopyanov KL, Kulevsky LA, Mikhalevich VG, Rodin AM. Laser-induced generation of subnanosecond sound pulses in liquids. *Sov. Phys. JETP* 1986; **91**: 114-121.

7. Sigrist MW. Laser generation of acoustic waves in liquids and gases. *J. Applied Phys.* 1986; **60**: R83-R121.

8. Emmony DC. Interaction of IR laser radiation with liquids. *Infrared Phys.* 1985; **25**: 133-139.

9. Cleary SF, Hamrick PE. Laser-induced acoustic transients in mammalian eye. *J. Acoust. Soc. Am..* 1969; **46**(4): 1037-1044.

10. Cleary SF. Laser pulsed generation of acoustic transients in biological materials, In: "Laser applications in Medicine and Biology", Vol.3, Plenum Press, New York, 1977, pp. 175-219.

11. Vogel A, Busch S, Asiyo-Vogel M : Time-resolved measurements of shock wave emission and cavitation bubble generation in intraocular laser surgery with ps and ns pulses and related tissue effects. *Proc. SPIE* (Europe'92) Budapesht, Hungary.

12. Esenaliev RO, Oraevsky AA, Letokhov VS, Karabutov AA, Malinsky TV: Studies of acoustic and shock waves in the pulsed laser ablation of biological tissue. *Lasers Surg. Med.* 1993; **13**: 470-484.

13. Bunkin NF, Bunkin FV : New concepts in the optical breakdown of transparent liquids. *Laser Physics* 1993; **3**(1): 63-78.

14. Goss SA, Johnston RL, Dunn F : Comprehensive compilation of empirical ultrasonic properties of mammalian tissues, *J. Acoustic Soc. Am.* 1978; **64**(2): 423-457.

15. Docchio F, Regondi P. Capon M, Mellerio J : Study of temporal and spatial dynamics of plasmas induced in liquids by nanosecond Nd:YAG laser pulses. *Appl. Opt.* 1988; **27**(7): 3661-3674.

16. Blankenstein MF, Zuclich JA, Allen RG: Retinal hemorrhage thresholds for Q-switched Nd:YAG laser exposures. *Invest Ophthalmic.* 1986; **27**(7): 1176-1179.

17. Marshall J. Structural aspects of laser-induced damage and their functional implications. *Health Phys.* 1989; **56**(5): 617-624.

18. Vogel A, Schweiger P, Frieser A: Intraocular Nd:YAG laser surgery. Light-tissue interaction, damage range and reduction of collateral effects. *IEEE J. Quant. Electron.* 1990; **26**(11): 2240-2258.

19. Naugolnykh KA, Roi NA. "Electrical discharges in water." Moscow, Nauka, 1971

20. Avdeev PS, Berezin Yu.D., Volkov VV et al. Biological action of laser infrared radiation with 1064-nm wavelength on retina tissue. *Vestnik Ophthalmol.* 1982; **1**: 26-30.

21. Cole RL: "Underwater Explosions", Dover Publishers, New York 1965.

22. Jones DL: Intermediate strength blast wave. *Phys. Fluids* 1968; **11**(8): 1664-1667.

23. Joffe A, Melnikov NA, Naugolnikh KA, Upadyshev VA: Shock wave under optical breakdown in water. *J. Appl. Mech. and Tech. Phys.* 1970; **3**: 125-127.

24. Feslenko VS: An investigation of light-acoustic and light-hydrodynamic parameters of the laser breakdown in liquids. *Sov. J. Quant. Electron.* 1977; **4**(8): 1732-1737.

25. Teng P, Nishioka NS, Anderson RR, Deutsch TF: Acoustic studies of the role of immersion in plasma-mediated laser ablation. *IEEE J. Quant. Electron.* 1987; **23**(10): 1845-1852.

26. Campillo AJ, Griffin RD, Schoen PE: Reflective probing of laser-generated multi-kilobar compression shocks in water. *Opt. Comm.* 1986; **57**(5): 301-307.

27. Doukas A, Zweig AD, Frisoli JK, Birngruber R, Deutsch TF: Non-invasive determination of shock wave pressure generated by optical breakdown. *Appl. Phys. B* 1991: **53**: 237-245.

28. Oraevsky AA, Esenaliev RO, Letokhov VS: Temporal characteristics and mechanism of atherosclerotic tissue ablation by nanosecond and picosecond laser pulses, *Lasers Life Sci.* 1992; **5**(1-2): 75-93.

29. Skripov VP: "Metastable Liquids" John Willey & Songs, New York, 1974.

30. Reid RC: American Scientist 1976; **64**: 146.

31. Pustovalov VK Thermal processes under the action of laser radiation pulse on absorbing granules in heterogeneous biotissues. *Int. J. Heat Mass Transfer* 1993; **36**(2): 391-399.

32. Golubnichiy PI, Kalushyi GS, Korchikov SD: Sound generated by laser beam propagation in liquid with particles. *J. Appl. Mech. Tech. Phys.* 1984; **1**: 9-12.

33. Landau LD, Lifshitz EM: "Fluid Mechanics", Pergamon Press, Oxford, 1959.